Steric Influence on the Structure, Magnetic Properties, and Reactivity of Hexa- and Octaisopropylmanganocene

Melanie L. Hays,[†] David J. Burkey,[†,⊥] Jason S. Overby,[†] Timothy P. Hanusa,*[,†] Scott P. Sellers,[‡] Gordon T. Yee,[‡] and Victor G. Young, Jr.[§]

Department of Chemistry, Vanderbilt University, Nashville, Tennessee 37235, Department of Chemistry and Biochemistry, University of Colorado at Boulder, Boulder, Colorado 80309, and Department of Chemistry, University of Minnesota, Minneapolis, Minnesota 55455

Received July 14, 1998

The reaction of KCp^{ni} ($Cp^{ni} = (C_3H_7)_nC_5H_{5-n}$; $n = 3$, 4) with $MnCl_2$ in THF produces the metallocenes $(Cp^{3i})_2Mn$ or $(Cp^{4i})_2Mn$ in good yield. Solid-state magnetic susceptibility measurements indicate that orange-red $(Cp^{3i})_2Mn$ is in high-spin/low-spin equilibrium at room temperature. In the solid-state, it has a centrosymmetric sandwich structure with an average Mn−C bond length (2.130(6) Å) typical of low-spin manganocenes. $(Cp^{3i})_2Mn$ reduces tetracyanoethylene (TCNE) to generate the TCNE radical anion. Despite the presence of additional electron-donating isopropyl groups, pale yellow $(Cp^{4i})_2Mn$ is entirely high-spin from room temperature to 10 K. The crystal structure of $(Cp^{4i})_2Mn$ reveals a bent metallocene structure, with a centroid−Mn−centroid angle of 167.4° and an average Mn−C distance of 2.42(2) Å. This structure is consistent with its high-spin electron configuration; the longer Mn−C bonds provide relief from the steric strain that would be present in a low-spin complex. The reaction of $(Cp^{4i})_2Mn$ with TCNE produces a tricyanovinylation product, $C_5(i\text{-Pr})_4HC(CN)=C(CN)_2$, which was characterized by X-ray diffraction.

Introduction

The magnetic properties of most transition metal compounds subject to spin-state crossovers can be analyzed successfully in terms of temperature, pressure, solvent, lattice characteristics (for solids), and the electronic properties of their associated ligands.[1] In addition, a variety of iron coordination complexes containing N-donor ligands such as diimines,[2] poly(pyrazoyl)borates,[3] or substituted pyridines[4] are known in which inter- or intraligand steric crowding and the associated bond length changes affect the relative stability of the metal spin states. In some cases, the addition of only one methyl group (e.g., the difference between tris(2-pyridylmethyl)amine (TPA) and (6-methyl)TPA) is enough to favor the high-spin configuration of a complex.[4] In contrast, probably because of the prevalence of strong π-acceptor ligands that support low-spin states (e.g., CO, PR_3, Cp), steric influence on magnetic properties has been difficult to demonstrate in an *organometallic* complex.

Among first-row metallocenes, manganocenes are unique in having two energetically accessible spin states that can be readily interconverted by the electronic properties of the cyclopentadienyl ligands. Electron-donating substituents on the rings (e.g., alkyls) support a low-spin ($^2E_{2g}$) configuration, whereas less electropositive groups (e.g., H, $SiMe_3$) favor a high-spin ($^6A_{1g}$) state. For example, at room-temperature Cp_2Mn and $(Me_3SiC_5H_4)_2Mn$ are almost entirely high-spin;[5−7] however, $(MeC_5H_4)_2Mn$ exists as a nearly equal mixture of low-spin and high-spin complexes,[5,7] and the fully methylated derivative Cp^*_2Mn is exclusively low-spin at this temperature.[8,9] The low-spin complexes have shorter (ca. 2.1 Å), more covalent and less reactive Mn−C bonds (e.g., Cp^*_2Mn is stable for several hours in water), whereas the high-spin complexes have longer Mn−C bonds (ca. 2.4 Å) that are more reactive and "ionic" in character (Cp_2Mn decomposes on contact with water).

Our interest in the chemistry of main-group[10−12] and transition-metal[13] metallocenes containing highly substituted, "encapsulating" cyclopentadienyl rings led us to examine the influence of such ligands on manga-

[†] Vanderbilt University.
[‡] University of Colorado at Boulder.
[§] University of Minnesota.
[⊥] Present address: Department of Chemistry, San Diego State University, San Diego, CA.

(1) König, E.; Ritter, G.; Kulshreshta, S. K. *Chem. Rev.* **1985**, *85*, 219−234.
(2) Goodwin, H. A. *Coord. Chem. Rev.* **1976**, *18*, 293−325.
(3) Sohrin, Y.; Kokusen, H.; Matsui, M. *Inorg. Chem.* **1995**, *34*, 3928−3934.
(4) Zang, Y.; Kim, J.; Dong, Y.; Wilkinson, E. C.; Appelman, E. H.; Que, L., Jr. *J. Am. Chem. Soc.* **1997**, *119*, 4197−4205.
(5) Switzer, M. E.; Wang, R.; Rettig, M. F.; Maki, A. H. *J. Am. Chem. Soc.* **1974**, *96*, 7669−7674.
(6) Ammeter, J. H.; Bucher, R.; Oswald, N. *J. Am. Chem. Soc.* **1974**, *96*, 7833−7835.
(7) Hebendanz, N.; Köhler, F. H.; Müller, G.; Riede, J. *J. Am. Chem. Soc.* **1986**, *108*, 3281−3289.
(8) Robbins, J. L.; Edelstein, N. M.; Cooper, S. R.; Smart, J. C. *J. Am. Chem. Soc.* **1979**, *101*, 3853−3857.
(9) Smart, J. C.; Robbins, J. L. *J. Am. Chem. Soc.* **1978**, *100*, 3936−3937.
(10) Williams, R. A.; Tesh, K. F.; Hanusa, T. P. *J. Am. Chem. Soc.* **1991**, *113*, 4843−4851.
(11) Burkey, D. J.; Hanusa, T. P. *Organometallics* **1995**, *14*, 11−13.
(12) Burkey, D. J.; Hanusa, T. P. *J. Organomet. Chem.* **1996**, *512*, 165−173.
(13) Burkey, D. J.; Hays, M. L.; Duderstadt, R. E.; Hanusa, T. P. *Organometallics* **1997**, *16*, 1465−1475.

10.1021/om980596n CCC: $15.00
Publication on Web 11/10/1998

nocenes. We found preliminary evidence that $(Cp^{4i})_2$-Mn ($Cp^{4i} = (C_3H_7)_4C_5H$) displays high-spin magnetic behavior in solution despite the presence of alkyl groups that should stabilize the low-spin state.[14] While this work was in progress, Sitzmann reported the synthesis and solid state magnetic behavior of several highly substituted manganocenes, including $(Cp^{4i})_2Mn$, which confirmed the solution data.[15] We report here the solid-state structure of $(Cp^{4i})_2Mn$, along with the structure and magnetic behavior of the related manganocene $(Cp^{3i})_2Mn$. These data provide further insight into the role that the steric demands of the ligands can have on the magnetic properties of susceptible metallocenes.

Experimental Section

General Considerations. All manipulations were performed with the rigorous exclusion of air and moisture using high-vacuum, Schlenk, or drybox techniques. Proton NMR spectra were obtained on a Bruker NR-300 spectrometer at 300 MHz, and were referenced to the residual proton resonances of C_6D_6 (δ 7.15). Infrared data were obtained with KBr pellets that were prepared as previously described.[10] UV−vis and ESR spectra were obtained on Shimadzu UV-2101PC and Bruker ESP 300 ESR spectrometers, respectively. Elemental analyses were performed by Oneida Research Services, Whitesboro, NY.

Materials. Nominally anhydrous manganese(II) chloride (Aldrich) was heated under vacuum (150 °C, 10^{-6} Torr) to ensure the complete removal of coordinated water. KCp^{3i} ($[Cp^{3i}]^- = 1,2,4\text{-}(C_3H_7)_3C_5H_2$) and KCp^{4i} ($[Cp^{4i}]^- = 1,2,3,4\text{-}(C_3H_7)_4C_5H$) were prepared as previously described.[10] Tetracyanoethylene (TCNE) was purchased from Aldrich and purified by sublimation under vacuum. Solvents for reactions were distilled under nitrogen from sodium or potassium benzophenone ketyl.[16] C_6D_6 and THF-d_8 were vacuum distilled from Na/K (22/78) alloy and stored over 4A molecular sieves prior to use.

Magnetic Measurements. Magnetic moment measurements were performed on a 5 T Quantum Design MPMS-5 SQUID magnetometer in a field of 5000 G. Magnetization as a function of field was also measured to check for ferromagnetic impurities; none were found. To handle these extremely air-sensitive compounds, a sample holder was constructed from segments of a 5 mm diameter 507 NMR tube.[17] The sample (~25 mg) was placed into the tube in the glovebox, and the tube was packed with a small piece of glass wool (~10 mg). The tube was attached to a Teflon stopcock by means of an UltraTorr connector. It was then taken from the glovebox and flame sealed under dynamic vacuum. The diamagnetic correction for each complex was estimated from Pascal's constants. The diamagnetic susceptibility of the glass wool was calculated from its mass and previously measured average gram susceptibility. The diamagnetic susceptibility of the sample holder was taken to be the average value of measurements on several identical sample holders.

Synthesis of $(Cp^{3i})_2Mn$. An Erlenmeyer flask was charged with KCp^{3i} (0.58 g, 2.5 mmol) and $MnCl_2$ (0.16 g, 1.3 mmol); to this was added 25 mL of THF. The reaction mixture was stirred for 16 h, during which time the solution changed from pale yellow to deep red. The THF was removed under vacuum, and the orange-red residue was extracted with 40 mL of hexanes. Filtration removed a yellow precipitate and gave a blood-red hexanes filtrate. Removal of the hexanes under vacuum from the filtrate and fractional sublimation of the remaining solid (90−100 °C, 10^{-6} Torr) gave 0.34 g (62% yield) of $(Cp^{3i})_2Mn$ as an air-sensitive, red-orange powder (mp 116−118 °C). Anal. Calcd for $C_{28}H_{46}Mn$: C, 76.85; H, 10.60. Found: C, 76.49; H, 10.20. ^{1}H NMR (C_6D_6): δ 10.1 ($\omega_{1/2}$ = 300 Hz); −0.7 ($\omega_{1/2}$ = 400 Hz); −10.7 ($\omega_{1/2}$ = 1000 Hz); the relative intensities of the resonances are ca. 2:2:1. Principal IR bands (KBr, cm^{-1}): 3087 (w), 2946 (s, br), 2920 (sh), 2868 (sh), 1459 (s), 1434 (sh), 1374 (s), 1356 (s), 1326 (m), 1270 (s), 1178 (s), 1150 (w), 1102 (m), 1085 (sh), 1048 (s), 1020 (s), 944 (s), 920 (m), 838 (s), 798 (m), 724 (m), 686 (w), 585 (w), 478 (m). UV−vis (THF, λ in nm; ϵ in L mol^{-1} cm^{-1}): λ_{max} 222 (11 881), 242 (10 629), 446 (605).

Reaction of $(Cp^{3i})_2Mn$ with TCNE. Tetracyanoethylene (0.081 g, 0.63 mmol) was dissolved in 20 mL of acetonitrile. $(Cp^{3i})_2Mn$ (0.315 g, 0.72 mmol) was added with stirring. The solution was heated to boiling and then removed from the heat and allowed to stand for 18 h without stirring. The solvent was then removed by rotary evaporation, and the organic byproducts were extracted into hexanes. The extract was filtered, leaving a brownish solid (0.141 g) that turned olive green after drying under vacuum (mp > 250 °C). Satisfactory elemental analysis was not obtained for the formula $(Cp^{3i})_2$-Mn[TCNE] although the UV−vis and ESR spectra (see below) are characteristic of the TCNE radical anion.[18] UV−vis (MeCN, ϵ): λ_{max} 207 (11,608), 231 (8872), 383 (2821), 390 (3032), 398 (3329), 407 (3639), 417 (3977), 427 (4104), 437 (4217), 446 (4175), 459 (3963), 469 (3639). The solid did not have enough solubility in C_6D_6, THF-d_8, or MeCN-d_3 to obtain an NMR spectrum.

Synthesis of $(Cp^{4i})_2Mn$. KCp^{4i} (0.49 g, 1.80 mmol) and $MnCl_2$ (0.11 g, 0.90 mmol) were combined in 20 mL of THF in an Erlenmeyer flask; the light-yellow suspension was stirred for 18 h. The THF was then removed by rotary evaporation under vacuum, and the pale yellow residue was extracted with 25 mL of hexanes. Subsequent filtration of the mixture and removal of the hexanes from the filtrate under vacuum left a yellow residue. Recrystallization from 5 mL of THF at room temperature allowed for the isolation of 0.36 g (77% yield) of $(Cp^{4i})_2Mn$ as a light yellow, crystalline solid (mp 226−228 °C). Anal. Calcd for $C_{34}H_{58}Mn$: C, 78.27; H, 11.20; Mn, 10.53. Found: C, 75.48; H, 11.11; Mn, 10.07. The unsatisfactory analysis for carbon may be a consequence of the compound's high air-sensitivity and/or limited thermal stability. ^{1}H NMR (C_6D_6): δ 25.6 (ω_H = 2500 Hz); 21.5 (ω_H = 5100 Hz). Principal IR bands (KBr, cm^{-1}): 2956 (s, br), 2888 (sh), 1460 (s), 1420 (w), 1376 (s), 1365 (s), 1327 (w), 1310 (w), 1260 (w), 1176 (m), 1146 (w), 1102 (m), 1084 (w), 1060 (w), 1034 (w), 980 (m), 775 (m), 676 (w), 607 (w), 519 (w), 505 (m). UV−vis (THF, λ in nm; ϵ in L mol^{-1} cm^{-1}): λ_{max} 223 (9237) shoulder, 270 (6316), 353 (989). $(Cp^{4i})_2Mn$ is highly air and moisture sensitive; crystalline samples of the complex decompose immediately on contact with the atmosphere.

Synthesis of $C_5(i\text{-}Pr)_4HC(CN)=C(CN)_2$ from $(Cp^{4i})_2Mn$ and TCNE. TCNE (0.056 g, 0.44 mmol) was dissolved in 25 mL of acetonitrile, and $(Cp^{4i})_2Mn$ (0.113 g, 0.217 mmol) was added with stirring. The solution was heated to boiling and then removed from the heat and allowed to stand for 18 h without stirring. The solvent was then removed by rotary evaporation, and the organic product was extracted into hexanes. The hexanes solution was filtered, and the filtrate was retained. A small amount (17 mg) of an unidentified light orange solid ($Mn(CN)_2$?) was collected on the frit of the funnel. The hexanes was removed from the filtrate, and the remaining red solid was dried under vacuum (0.115 g, 79% yield) (mp 82−83 °C). ^{1}H NMR (C_6D_6): δ 4.29 (s, 1 H, ring-C*H*); 2.65−2.80 (two overlapping septets, 3 H, C*H*Me$_2$); 1.05 (apparent

(14) Hays, M. L.; Hanusa, T. P. *Adv. Organomet. Chem.* **1996**, *40*, 117−170.
(15) Sitzmann, H.; Schär, M.; Dormann, E.; Keleman, M. *Z. Anorg. Allg. Chem.* **1997**, *623*, 1609−1613.
(16) Perrin, D. D.; Armarego, W. L. F. *Purification of Laboratory Chemicals*, 3rd ed.; Pergamon: Oxford, 1988.
(17) Quantum Design Application Note no. 1, Sample Mounting.
(18) Phillips, W. D.; Rowell, J. C. *J. Chem. Phys.* **1960**, *33*, 626−627.

Table 1. Crystal Data and Summary of Data Collection for $(Cp^{3i})_2Mn$

formula	$C_{28}H_{46}Mn$
fw	437.61
cryst color	orange-red
cryst dimens (mm)	0.55 × 0.40 × 0.38
space group	$P\bar{1}$
cell dimens (20 °C)	
a (Å)	9.116(1)
b (Å)	9.3585(6)
c (Å)	8.828(1)
α (deg)	100.605(9)
β (deg)	117.710(8)
γ (deg)	76.342(8)
V (Å^3)	645.6(1)
Z	1
calcd density (g/cm^3)	1.125
abs coeff (mm^{-1})	4.22
F(000)	239
scan speed (deg/min)	8.0
scan width	1.68 + 0.30 tan *θ*
limits of data collection	$6.0° \le 2\theta \le 120.1°$
index ranges	$0 \le h \le 10$, $-11 \le k \le 11$, $-10 \le l \le 10$
total reflns	2059
unique reflns	1920
refinement method	full-matrix least-squares on *F*
R indices ($I > 3\sigma(I) = 1735$)	$R = 0.040$, $R_w = 0.049$
GOF on *F*	1.93
maximum Δ/σ in final cycle	0.56
max/min peak in final diff map	0.29/−0.32 e$^-$/Å^3

triplet, $J = 7.0$ Hz, 12 H, C*H*$_3$); 0.85 (dd, $J = 7.0$ Hz, $J = 11.6$ Hz, 12 H, C*H*$_3$). ^{13}C NMR (C_6D_6) δ 203.9 (−(CN)*C*═C(CN)$_2$); 154.9 (ring-*C*CHMe$_2$); 152.0 (ring-*C*CHMe$_2$); 112.7 (*C*N); 110.8 (*C*N); 110.4 (*C*N); 98.1 (═*C*(CN)2); 53.7 (ring-*C*H); 28.2 (*C*HMe$_2$); 27.0 (*C*HMe$_2$); 22.6 (*C*H$_3$); 20.6 (*C*H$_3$). Principal IR bands (KBr, cm^{-1}): 2965 (s), 2934 (m), 2873 (m), 2235 (w), 2224 (w), 1460 (m), 1384 (m), 1367 (m), 1262 (s), 1097 (s), 1021 (s), 802 (s), 613 (m), 601 (m), 460 (m). UV−vis (THF, ϵ): λ_{max} 214 (5168), 268 (8286), 326 (723), 474 (1151).

X-ray Crystallography. A. $(Cp^{3i})_2Mn$. Several attempts at X-ray structural determination of $(Cp^{3i})_2Mn$ from crystals grown from either THF or hexanes were unsuccessful owing to extensive twinning. However, crystals grown from toluene at room temperature did not suffer from this problem, and one of these was used for data collection. A suitable crystal was located and sealed in a glass capillary tube. Measurements were performed on a Rigaku AFC6S diffractometer at Vanderbilt University with graphite-monochromated Cu Kα radiation ($\lambda = 1.541\,78$ Å). Relevant crystal and data collection parameters for the compound are given in Table 1.

A set of diffraction maxima corresponding to a triclinic cell was found from a systematic search of a limited hemisphere of reciprocal space; the space group $P\bar{1}$ was initially chosen from a consideration of unit cell parameters. Subsequent solution and refinement of the structure was consistent with the choice.

Data collection was performed using continuous $\omega-2\theta$ scans with stationary backgrounds (peak/bkgd counting time = 2:1). No decay was evident in the intensities of three representative reflections measured after every 150 reflections. Data were reduced to a unique set of intensities, and associated σ values in the usual manner. The structure was solved by direct methods (SHELXS-86, DIRDIF) and Fourier techniques.

The manganese atom in the complex is located on a crystallographically imposed inversion center. The hydrogen atoms were identified in difference Fourier syntheses and were refined isotropically in the final least-squares cycles. Final difference maps were featureless. Selected bond distances and angles are listed in Table 3.

B. $(Cp^{4i})_2Mn$. Data collection and structure solution were conducted at the X-ray Crystallographic Laboratory at the University of Minnesota. The specimen used for data collection was cut from a large hexagonal plate grown from toluene. This specimen was composed of a multiplicity of smaller plates. The sample was later determined to possess a twin (about 12% of the specimen), but this did not hinder the solution of the structure. The crystal was attached to a glass fiber and mounted on a Siemens SMART Platform CCD system for a data collection at 173(2) K. An initial set of cell constants was calculated from reflections harvested from three sets of 20 frames. These initial sets of frames were oriented such that orthogonal wedges of reciprocal space were surveyed. This produced orientation matrixes determined from 41 reflections. Final cell constants were calculated from a set of 5359 strong reflections from the actual data collection. All calculations were performed using SGI INDY R4400−SC or Pentium computers using the SHELXTL V5.0 suite of programs. Relevant crystal and data collection parameters for the

Table 2. Crystal Data and Summary of X-ray Data Collection for $(Cp^{4i})_2Mn$

formula	$C_{34}H_{58}Mn$
fw	521.74
cryst color	yellow
cryst dimens (mm)	0.25 × 0.20 × 0.16
space group	*C*2/*c*
cell dimens (173 ± 2 K)	
a (Å)	16.2998(9)
b (Å)	16.8944(9)
c (Å)	23.4009(13)
β (deg)	92.322(1)
V (Å^3)	6438.7(6)
Z	8
calcd density (g/cm^3)	1.076
abs coeff (mm^{-1})	0.428
F(000)	2296
limits of data collection	$1.74° \le \theta \le 25.38°$
index ranges	$-19 \le h \le 19$, $-20 \le k \le 20$, $0 \le l \le 27$
total reflns	15175
unique reflns	5579 ($R_{int} = 0.0566$)
refinement method	full-matrix least-squares on F^2
weighting scheme	$w = [\sigma^2(F_0^2) + (AP)^2 + (BP)]-1$, where $P = (F_0^2 + 2F_c^2))/3$, $A = 0.0741$, and $B = 4.6965$
abs corr	SADABS (Sheldrick, 1996)
max and min transmn	1.000 and 0.694
data/restraints/parameters	5065/0/339
R indexes ($I > 2\sigma(I) =$ 3160)	R1 = 0.0780, wR2 = 0.1570
R indexes (all data)	R1 = 0.1515, wR2 = 0.1886
GOF on F^2	1.061
max/min peak (final diff map)	0.581/−0.410 e$^-$/Å^3

Table 3. Selected Bond Distances (a) and Angles (deg) for $(Cp^{3i})_2Mn$

atoms	distance	atoms	distance
Mn(1)−C(2)	2.151(3)	C(2)−C(7)	1.509(4)
Mn(1)−C(3)	2.119(3)	C(4)−C(10)	1.507(4)
Mn(1)−C(4)	2.127(3)	C(5)−C(13)	1.509(4)
Mn(1)−C(5)	2.131(3)	C(7)−C(8)	1.474(7)
Mn(1)−C(6)	2.123(3)	C(7)−C(9)	1.485(7)
Mn(1)−ring centroid	1.755	C(10)−C(11)	1.523(5)
C(2)−C(3)	1.412(4)	C(10)−C(12)	1.523(6)
C(2)−C(6)	1.415(4)	C(13)−C(14)	1.531(5)
C(3)−C(4)	1.423(4)	C(13)−C(15)	1.514(6)
C(4)−C(5)	1.425(4)		
C(5)−C(6)	1.426(4)		

$CH_3-CH-CH_3$ (av)	110.5(6)°
planarity of rings	within 0.003 Å
ring centroid−Mn(1)−ring centroid	180°
ring normal−Mn(1)−ring normal	180°
av displacement of methine carbon from ring plane	0.10 Å

Table 4. Selected Bond Lengths (Å) and Angles (deg) for $(Cp^{4i})_2Mn$

atoms	distance	atoms	distance
Mn(1)−C(1)	2.388(5)	C(1)−C(2)	1.380(7)
Mn(1)−C(2)	2.447(5)	C(1)−C(5)	1.406(7)
Mn(1)−C(3)	2.450(5)	C(2)−C(3)	1.442(7)
Mn(1)−C(4)	2.419(5)	C(3)−C(4)	1.460(7)
Mn(1)−C(5)	2.395(5)	C(4)−C(5)	1.436(6)
Mn(1)−C(18)	2.380(5)	C(18)−C(19)	1.393(6)
Mn(1)−C(19)	2.407(5)	C(18)−C(22)	1.415(6)
Mn(1)−C(20)	2.414(5)	C(19)−C(20)	1.448(7)
Mn(1)−C(21)	2.432(5)	C(20)−C(21)	1.440(7)
Mn(1)−C(22)	2.443(5)	C(21)−C(22)	1.415(6)
C(ring)−CH (av)	1.52(2)	CH−CH_3 (av)	1.52(3)
CH_3−CH−CH_3 (av)		112(1)°	
planarity of rings		within 0.010 Å	
ring centroid−Mn(1)−ring centroid		167.4°	
av displacement of methine carbon from ring plane		0.19 Å	

compound are given in Table 2, and selected bond distances and angles are listed in Table 4.

A hemisphere data collection technique was used for this specimen. A randomly oriented region of reciprocal space was surveyed to the extent of 1.3 hemispheres to a resolution of 0.84 Å. Three major swaths of frames were collected with 0.30 steps in ω.

The space group *C*2/*c* was determined on the basis of systematic absences and intensity statistics. A successful direct-methods solution was calculated which provided most non-hydrogen atoms from the E-map. Several full-matrix least squares/difference Fourier cycles were performed that located the remainder of the non-hydrogen atoms. All non-hydrogen atoms were refined with anisotropic displacement parameters. All hydrogen atoms were placed in ideal positions and refined as riding atoms with relative isotropic displacement parameters.

In the final stages of refinement, it was observed that the 50 worst reflections all had low *l* indices. Inspection of several of these reflections and their twin components confirmed the presence of the pseudo-merohedral type twin encountered when β is near 90°. The data were modified to produce an "HKLF 5" type SHELX reflection file with a locally written program UNTWIN (UNTWIN, Victor G. Young, Jr., The University of Minnesota). All reflections with *l* indices between −6 and 6 have significant twinning. Each reflection was paired with its twin as determined by UNTWIN and the batch scale factor (increased accordingly to the *l* index). The reflections at $l = 0$ have exact overlaps with their twin. However, as the absolute value of the $l = 0$ index increases, the reflections from both twins separate in reciprocal space. The separation at $l = 1$ is about 0.001 95. Ascension to higher layers increase the separation by the same amount for each successive step. Once the $l = 7$ index is obtained, there is no longer any significant overlap. The extent of overlap was refined by the addition of seven additional batch scale factors, one for each layer of absolute value in *l*. The refinement using this model is 1.2% better than that without modeling twinning. Both models have data truncated at a resolution higher than 0.87 Å owing to the dearth of observed reflections in that region. Information corresponding to the untwinned refinement is not included here.

Results

Synthesis of $(Cp^{3i})_2Mn$ and $(Cp^{4i})_2Mn$. Reaction of 2 equiv of either KCp^{3i} or KCp^{4i} with $MnCl_2$ in THF yielded the corresponding metallocenes $(Cp^{3i})_2Mn$ and $(Cp^{4i})_2Mn$ in good yield (eq 1)

$$2KCp^{ni} + MnCl_2 \xrightarrow{THF} (Cp^{ni})_2Mn + 2KCl\downarrow \quad n = 3,4 \qquad (1)$$

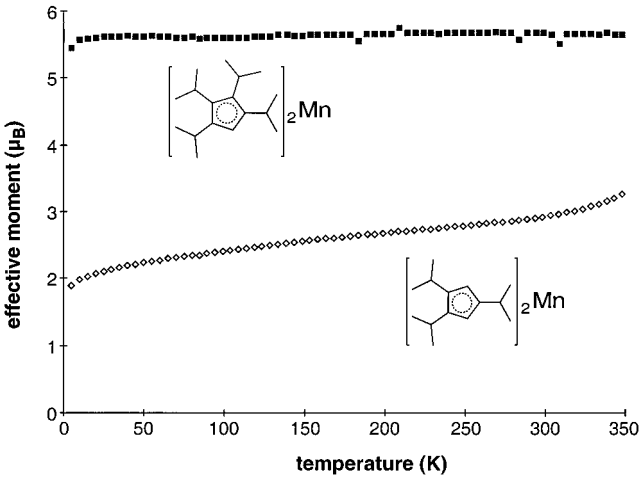

Figure 1. Magnetic moment as a function of temperature for $(Cp^{3i})_2Mn$ and $(Cp^{4i})_2Mn$ in a field of 5000 G. $(Cp^{3i})_2Mn$ displays evidence of spin equilibrium, whereas the magnetic moment of $(Cp^{4i})_2Mn$ is temperature independent to 10 K.

The products were extracted from the reaction mixture with hexanes; purification was accomplished by either fractional sublimation or recrystallization from THF. $(Cp^{3i})_2Mn$ was isolated as an orange-red powder, and formed deep red crystals, whereas $(Cp^{4i})_2Mn$ was obtained as a pale-yellow solid, and formed almost colorless crystals.

$(Cp^{3i})_2Mn$ displays air-sensitivity similar to that reported for Cp^*_2Mn;[8,9] crystalline samples decompose slowly over a few minutes in air, but solutions of the complex decompose rapidly. $(Cp^{4i})_2Mn$ is more air-sensitive than $(Cp^{3i})_2Mn$, as solid samples of $(Cp^{4i})_2Mn$ decompose instantly on exposure to the atmosphere. Samples of both manganocenes also underwent significant decomposition on standing under nitrogen atmosphere at room temperature, noticeable decomposition usually occurring after approximately 2 months for $(Cp^{3i})_2Mn$ and after a few weeks for $(Cp^{4i})_2Mn$. However, the latter is stable for at least a year at −2 °C.

Magnetic Susceptibility Measurements. Variable-temperature magnetic susceptibility measurements (186−353 K) with Evans' NMR method[19−22] on $(Cp^{3i})_2Mn$ reveal that the complex is mostly low-spin (2.32 μB) at 200 K; the value of the magnetic susceptibility gradually increases with temperature (e.g., 3.11 μ_B at 299 K). Comparable results are found in the solid state, as indicated by a plot of magnetic moment as a function of temperature (5−350 K) (Figure 1). The data indicate that an equilibrium or spin crossover exists between low-spin Mn^{II} at low temperature (1.89 μ_B at 5 K) and a higher spin species at elevated temperatures (e.g., 3.25 μ_B at 348 K). The asymptotic value of the magnetic moment at high temperature is above the range of the SQUID, but it seems reasonable that it represents a high-spin Mn^{II} species.

In marked contrast, the magnetic properties of $(Cp^{4i})_2Mn$ are clearly those of a *high-spin* species (Figure 1). In toluene, $(Cp^{4i})_2Mn$ exhibits Curie−Weiss behavior with an average magnetic moment of 5.73(±0.09) μ_B at all accessible temperatures (186−353 K). The magnetic moment is most consistent with high-spin Mn^{II}, which should be 5.92 μ_B, assuming $g = 2.00$. The magnetic moment is nearly temperature-independent down to 10 K; no strong antiferromagnetic coupling is observed. We observe a room-temperature value of 5.5 ± 0.1 μ_B (average of two determinations); Sitzmann has reported the higher value of 5.87 μ_B.[15]

Reactions and Properties of Manganocenes. Attempts to synthesize the sodium salts of $(Cp^{3i})_2Mn$ and $(Cp^{4i})_2Mn$ were unsuccessful, as reaction of either manganocene with sodium naphthalide in THF yielded only the sodium salts of $[Cp^{3i}]^-$ or $[Cp^{4i}]^-$. In contrast, $(Cp^{3i})_2Mn$ easily reduces tetracyano-

ethylene to form a charge-transfer salt (eq 2).

$$(Cp^{3i})_2Mn + TCNE \xrightarrow{MeCN} [(Cp^{3i})_2Mn]TCNE \qquad (2)$$

Although the solubility of $[(Cp^{3i})_2Mn]TCNE$ in MeCN-d_3 was too poor to obtain an ^1H NMR spectrum, its solubility in MeCN was high enough for UV−vis analysis. The spectrum is similar to the spectra of the TCNE charge-transfer salts of the decamethylmetallocenes.[23] Ten of the 17 vibrational overtones of $TCNE^{\bullet-}$ normally seen in this type of spectrum are apparent. Peaks for $[(Cp^{3i})_2Mn]^+$ are present at 207 and 231 nm in MeCN, shifted bathochromically from 222 and 242 nm in THF for the parent metallocene.

The ESR spectrum of $[(Cp^{3i})_2Mn]TCNE$ as a solid at 43 °C consists of only one broad resonance; however, the solution spectrum in acetonitrile at 27 °C contains 13 lines with a hyperfine coupling constant of 1.58(± 0.03) G. The spectrum is similar to the known spectrum of $[TCNE]^{\bullet-}$ that consists of 11 lines, nine of which are due to four equivalent ^{14}N with A^N = 1.56(± 0.02) G.[18] The other small resonances are believed to be a result of coupling with ^{13}C, which is in low abundance and has one of two coupling constants equal to $6A^N$.

The synthesis of the TCNE charge-transfer salt of $(Cp^{4i})_2Mn$ was attempted, but unlike the case with $(Cp^{3i})_2Mn$, a red hexanes-soluble compound was isolated. The compound was analyzed by NMR, IR, and UV−vis spectroscopies as well as by X-ray crystallography and determined to be the tricyanovinylation product $C_5(i\text{-}Pr)_4HC(CN)=C(CN)_2$ (eq 3). $(Cp^{4i})_2Mn$

$$(Cp^{4i})_2Mn + 2\,TCNE \xrightarrow{MeCN} 2 \qquad (3)$$

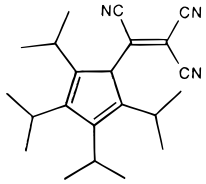

does not react with $FeCl_2$ to form the corresponding ferrocene, as do other high-spin complexes of manganocene.[24−26]

Solid State Structures. A. $(Cp^{3i})_2Mn$. After several unsuccessful attempts with crystals grown from hexanes or THF, a crystal of the complex grown from toluene was used to determine its structure by X-ray crystallography. $(Cp^{3i})_2Mn$ crystallizes in a triclinic unit cell with the manganese atom located at a crystallographically imposed inversion center; the cyclopentadienyl rings are thus parallel and perfectly staggered (twist angle of 36°). The complex is isomorphous with $(Cp^{3i})_2Fe$.[13] An ORTEP diagram of $(Cp^{3i})_2Mn$ is presented in Figure 2.

The average Mn−C bond distance in $(Cp^{3i})_2Mn$ is 2.130(6) Å, with a Mn−ring centroid distance of 1.755 Å. The average Mn−C bond length is similar to the analogous distances determined for the low-spin manganocenes Cp^*_2Mn[27] (2.114(2) Å) and $(MeC_5H_4)_2Mn$ (2.144(12) Å).[28,29] The $[Cp^{3i}]^-$ rings in $(Cp^{3i})_2Mn$ are slightly distorted from perfect pentahapto

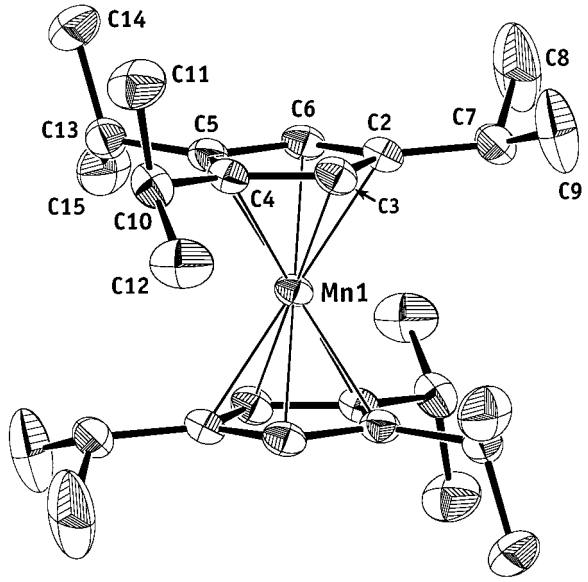

Figure 2. ORTEP plot of the non-hydrogen atoms of $(Cp^{3i})_2Mn$; thermal ellipsoids are displayed at the 30% level.

coordination; the Mn−C bond distances range from 2.119(3) Å for Mn(1)−C(3) to 2.151(3) Å for Mn(1)−C(2). Slight variations are also seen for the C−C bond distances in the cyclopentadienyl ring, which range from 1.412(4) to 1.426(4) Å. The presence of similar distortions in the structure of Cp^*_2Mn (i.e., an Mn−C range of 2.105(2)−2.118(2) Å and a C−C range of 1.409(2)−1.434(2) Å) was interpreted as an indication of a static Jahn−Teller distortion that relieves the orbital degeneracy of the ^2E_g ground state.[27] However, the distortions in $(Cp^{3i})_2Mn$ are most likely the result of the lower symmetry of this complex as compared to Cp^*_2Mn and are not due to a static Jahn−Teller distortion. This supposition is supported by the fact that similar variations in the M−C and C−C ring distances are seen in the structure of $(Cp^{3i})_2Fe$,[13] which is not subject to Jahn−Teller distortion.

The isopropyl substituents of $(Cp^{3i})_2Mn$ display orientations of 70.6°, 64.4°, and 19.3° relative to the ring plane. The latter, almost planar, orientation involves the C(7)−C(8)−C(9) isopropyl group, which has both methyl carbons tilted away from the manganese atom. This arrangement serves to minimize inter-ring contacts between the isopropyl groups; the closest inter-ring C···C contact is 4.03 Å (between C(9) and C(15)′) and is of little energetic significance.[30]

B. $(Cp^{4i})_2Mn$. Crystals of $(Cp^{4i})_2Mn$ were grown by slow evaporation of a saturated toluene solution. The compound crystallizes in the monoclinic space group *C*2/*c*. An ORTEP view of the molecule displaying the numbering scheme used in the tables is provided in Figure 3. $(Cp^{4i})_2Mn$ is a bent metallocene, with a centroid-Mn-centroid angle of 167.4°; this angle makes it the most bent of any neutral, monomeric transition metal metallocene.[14] The Mn−C distances range from 2.380(5) to 2.450(5) Å, which are consistent with a high-spin ground state, and are comparable to the Mn−C bond lengths in the high-spin manganocenes Cp_2Mn (2.380(6) Å),[31] $(MeC_5H_4)_2Mn$ (2.42(1) Å),[28,29] and $[(Me_3Si)C_5H_4]_2Mn$ (2.375(6) Å).[7] The Mn−C(ring) bond lengths for the unsubstituted carbon atoms in both rings of $(Cp^{4i})_2Mn$ are shorter than those of the isopropyl-substituted carbon atoms. An analogous pattern of M−C(ring) bond distances is found in the octaphenylmetallocenes $(Ph_4C_5H)_2M$.[32]

(19) Evans, D. F. *J. Chem. Soc.* **1959**, 2003−2005.
(20) Grant, D. H. *J. Chem. Educ.* **1995**, *72*, 39−40.
(21) Sur, S. K. *J. Magn. Reson.* **1989**, *82*, 169−173.
(22) Shubert, E. M. *J. Chem. Educ.* **1992**, *69*, 62.
(23) Dixon, D. A.; Miller, J. S. *J. Am. Chem. Soc.* **1987**, *109*, 3656−3664.
(24) Wilkinson, G.; Cotton, F. A.; Birmingham, J. M. *J. Inorg. Nucl. Chem.* **1956**, *2*, 95−113.
(25) Reynolds, L. T.; Wilkinson, G. W. *J. Inorg. Nucl. Chem.* **1954**, *9*, 86−92.
(26) Switzer, M. E.; Rettig, M. F. *J. Chem. Soc., Chem. Commun.* **1972**, 687−688.
(27) Freyberg, D. P.; Robbins, J. L.; Raymond, K. N.; Smart, J. C. *J. Am. Chem. Soc.* **1979**, *101*, 892−897.
(28) Almenningen, A.; Samdal, S.; Haaland, A. *J. Chem. Soc., Chem. Commun.* **1977**, 14−15.
(29) Almenningen, A.; Haaland, A.; Samdal, S. *J. Organomet. Chem.* **1978**, *149*, 219−229.
(30) Burman, J. A.; Hays, M. L.; Burkey, D. J.; Tanner, P. S.; Hanusa, T. P. *J. Organomet. Chem.* **1994**, *479*, 135−139.
(31) Haaland, A. *Inorg. Nucl. Chem. Lett.* **1979**, *15*, 267−269.
(32) Castellani, M. P.; Geib, S. J.; Rheingold, A. L.; Trogler, W. C. *Organometallics* **1987**, *6*, 1703−1712.

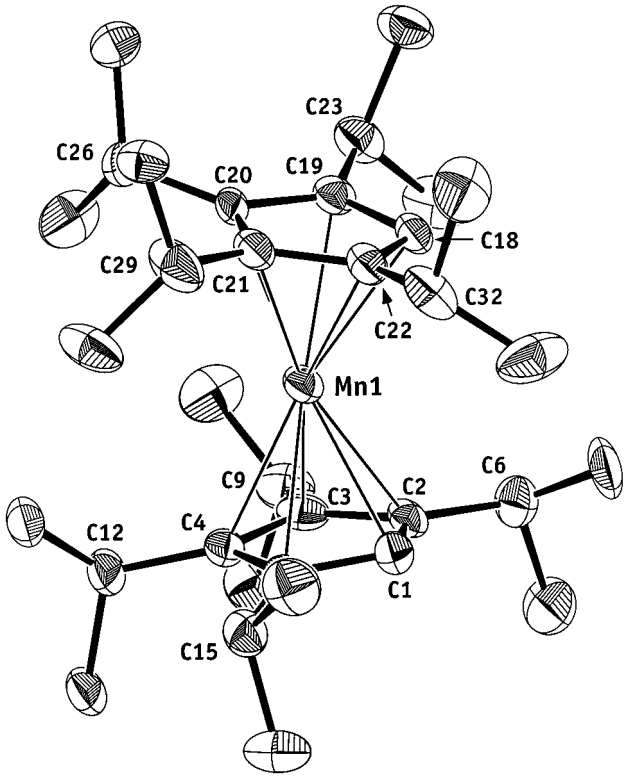

Figure 3. ORTEP plot of the non-hydrogen atoms of $(Cp^{4i})_2Mn$; thermal ellipsoids are shown at the 40% level.

Though not evident from the average bond parameters or the narrow range of Mn−C distances, there is considerable sterically induced displacements of the isopropyl substituents suggesting intramolecular strain. The average displacement of the isopropyl methine carbons from the cyclopentadienyl ring plane is 0.19 Å, though extreme values of 0.26 and 0.22 Å are found at C(15) and C(12), respectively. Even with the bending, there remain several intramolecular Me−Me′ contacts (e.g., C14···C27 at 3.70 Å) that are less than the sum of the van der Waals radii (4.0 Å).[33] These values emphasize the high steric requirements of the Cp^{4i} ligand.[34]

The intramolecular steric strain would be considerably higher, however, if the molecule maintained the Mn−Cp′ distances typical of a low-spin manganocene. Geometry optimization on $(Cp^{4i})_2Mn$ using semiempirical MO calculations (PM3) with the Mn−ring centroid distances initially constrained to that found in $(Cp^{3i})_2Mn$ (1.755 Å) suggests that there would be several inter-ring Me−Me′ contacts below 3.5 Å and one at 3.41 Å. Large displacements (up to 0.43 Å) of the isopropyl methine carbon atoms from the ring planes are also predicted to occur.[35]

C. $C_5(i\text{-}Pr)_4HC(CN)=C(CN)_2$. The compound crystallizes from toluene as small red needles. An ORTEP view of the molecule is provided in Figure 4; bond distances and angles of the complex are provided in the Supporting Information.

The geometric features are generally unremarkable. As is found in HCp^{4i} and many complexes containing the $[Cp^{4i}]^-$ anion, the isopropyl groups are oriented in a semi-geared arrangement.[36] The plane of the TCNE residue is perpendicular to that of the C_5 ring. The average C≡N bond length of 1.132(7) Å and the C=C length of 1.352(4) Å are the same within error as that in the cubic modification of TCNE (1.135(2) and 1.344(3) Å, respectively).[37]

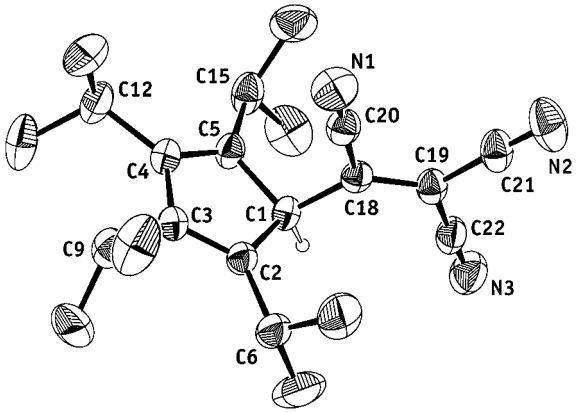

Figure 4. ORTEP diagram of $C_5(i\text{-}Pr)_4HC(CN)=C(CN)_2$, illustrating the numbering scheme used in the text. Thermal ellipsoids are shown at the 30% level.

Discussion

Methylation of cyclopentadienyl rings has consistently been found to favor the low-spin form of manganocenes. Manganocene itself is essentially high-spin at room temperature and above (5.50 μ_B at 373 K).[5,6,24,38] In contrast, gaseous 1,1′-$(MeC_5H_4)_2Mn$ is a mixture of both low- and high-spin states in almost equal proportions,[39] and $(Me_4C_5H)_2Mn$ is entirely low-spin up to 400 K.[7] Measurements on solid decamethylmanganocene indicate Curie behavior from 4 to 116 K with an effective magnetic moment of 2.16 ± 0.1 μ_B, while measurements by the Evans' method gave a magnetic moment of 1.97 ± 0.1 μ_B in toluene-d_8 at 313 K.[9]

Magnetic susceptibility measurements and X-ray data confirm that $(Cp^{3i})_2Mn$ continues the trend previously observed with the methylated manganocenes; i.e., the six electron-donating isopropyl substituents substantially stabilize the low-spin electronic ground state relative to Cp_2Mn. The slow increase in the magnetic moment with temperature suggests that the influence of the lattice is minimal, which may be a consequence of the heavily substituted cyclopentadienyl rings.[40] The reactivity of $(Cp^{3i})_2Mn$ is also consistent with a predominately low-spin state; like Cp^*_2Mn,[41] $(Cp^{3i})_2Mn$ readily reduces tetracyanoethylene in MeCN at room temperature to form a solid whose ESR spectrum in MeCN is characteristic of $[TCNE]^{\bullet-}$, although elemental analysis suggests that at least 60% of the $[Cp^{3i}]^-$ ligand has been lost. It should be noted that the TCNE salt of Cp^*_2Mn has limited stability at room temperature and is unstable in solution.

It might be expected that, like $(Me_4C_5H)_2Mn$,[7] $(Cp^{4i})_2Mn$ would be completely low-spin at room temperature.

(33) Pauling, L. *The Nature of the Chemical Bond*, 3rd. ed.; Cornell University Press: Ithaca, NY, 1960.
(34) Sitzmann, H.; Zhou, P.; Wolmershäuser, G. *Chem. Ber.* **1994**, *127*, 3−9.
(35) Unpublished results using the MacSpartan *Plus* package (Wavefunction, Inc., Irvine, CA).
(36) Burkey, D. J.; Alexander, E. K.; Hanusa, T. P. *Organometallics* **1994**, *13*, 2773−2786.
(37) Little, R. G.; Pautler, D.; Coppens, P. *Acta Crystallogr., Sect. B: Struct. Sci.* **1971**, *27*, 1493−1499.
(38) Cozak, D.; Gauvin, F. *Organometallics* **1987**, *6*, 1912−1917.
(39) Rabalais, J. W.; Werme, L. O.; Bergmark, T.; Karlsson, L.; Hussain, M.; Siegbahn, K. *J. Chem. Phys.* **1972**, *57*, 1185−1192.
(40) Gütlich, P.; Jung, J.; Goodwin, H. A. In *Molecular Magnetism: From Molecular Assemblies to the Devices*; Coronado, E., Delhaès, P., Gatteschi, D., Miller, J. S., Eds.; NATO ASI Series 321; Kluwer Academic: Dordrecht, The Netherlands, 1996; pp 327−378.
(41) Yee, G. T.; Manriquez, J. M.; Dixon, D. A.; McLean, R. S.; Groski, D. M.; Flippen, R. B.; Narayan, K. S.; Epstein, A. J.; Miller, J. S. *Adv. Mater.* **1991**, *3*, 309−311.

However, magnetic susceptibility measurements are clearly consistent with a temperature invariant high-spin state. The origin of the high-spin state in $(Cp^{4i})_2$-Mn evidently lies with the extreme bulk of the $[Cp^{4i}]^-$ ligand, which is sufficient to generate severe inter-ring steric strain.[13] Conversion of the hypothetical low-spin metallocene with ca. 2.1 Å Mn−C bonds to the high-spin state with Mn−C (av) of 2.42(2) Å partially relieves such crowding. The high-spin form of $(Cp^{4i})_2Mn$ then becomes the energetically preferred ground state. It is interesting to note that $[(t\text{-}Bu)_3C_5H_2]_2Mn$ is also high-spin, presumably for the same reasons;[15] its structure is not yet known.

The changes in spin state in $(Cp^{4i})_2Mn$ also influence its chemical reactivity. Rather than reduce TCNE, $(Cp^{4i})_2Mn$ undergoes a tricyanovinylation reaction, forming $C_5(i\text{-}Pr)_4HC(CN)=C(CN)_2$. Although generation of a similar product from a metallocene has not been observed before, tricyanovinylation reactions with neutral aromatic molecules have been well studied[42] and involve the initial formation of a π-complex followed by HCN elimination.[43] Thus, $(Cp^{4i})_2Mn$ appears to be a source of aromatic $[Cp^{4i}]^-$ anions in this reaction. Interestingly, however, $(Cp^{4i})_2Mn$ does not easily react with $FeCl_2$ as do other manganocenes.[24−26] This observation evidently reflects the steric shielding provided by the two rings, which serves to restrict access to the metal center and thus hinders ring exchange.

Conclusions

It is now clear that steric effects can be used to overrule the electronic preferences for spin-state in manganocenes, although this requires cyclopentadienyl rings with substantial steric demands (e.g., $[Cp^{4i}]^-$ or $[(t\text{-}Bu)_3C_5H_2]^-$ [15]). The contrasting chemical behavior of $(Cp^{3i})_2Mn$ and $(Cp^{4i})_2Mn$ clearly reflects the differences in the spin-states.

These complexes hint at the degree of control over magnetic properties that is possible in metallocenes through structural modifications of the cyclopentadienyl rings. Sterically influenced spin states in organometallic compounds may provide a source of stabilized high-spin building blocks for the study of charge-transfer phenomena or magnetic phase transitions.[44] The large number of available "supracyclopentadienyl" rings (i.e., $C_5R_nH_{5-n}$; n > 3; R > Me)[45] indicates that a rich area for exploration may lie here.

Acknowledgment. We thank Dr. Ron Goldfarb and the National Institute of Standards and Technology for the use of the SQUID magnetometers. D.J.B. is the grateful recipient of an NSF Predoctoral Fellowship. Acknowledgment is made to the donors of the Petroleum Research Fund, administered by the American Chemical Society, for partial support of this research (G.T.Y., T.P.H.).

Supporting Information Available: Atomic fractional coordinates, bond distances and angles, and anisotropic thermal parameters for $(Cp^{3i})_2Mn$, $(Cp^{4i})_2Mn$, and $C_5(i\text{-}Pr)_4HC(CN)=C(CN)_2$ (15 pages). See any current masthead page for ordering information.

OM980596N

(42) Fatiadi, A. J. *Synthesis* **1986**, 249−284.
(43) Nogami, T.; Nakano, Y.; Hasegawa, Y.; Shirota, Y.; Mikawa, H. *Bull. Chem. Soc. Jpn.* **1979**, *52*, 2110−2113.
(44) Broderick, W. E.; Thompson, J. A.; Day, E. P.; Hoffman, B. M. *Science* **1990**, *249*, 401−403.
(45) Janiak, C.; Schumann, H. *Adv. Organomet. Chem.* **1991**, *33*, 291−393.